

Changes in the flagellar bundling time account for variations in swimming behavior of flagellated bacteria in viscous media

Zijie Qu^{a,1}, Fatma Zeynep Temel^{a,b}, Rene Henderikx^{a,c}, and Kenneth S. Breuer^a

^aSchool of Engineering, Brown University, Providence, RI 02912; ^bSchool of Engineering and Applied Sciences, Harvard University, Cambridge, MA 02138; and ^cMicrosystems Group, Eindhoven University of Technology, Eindhoven 5600, The Netherlands

Edited by David A. Weitz, Harvard University, Cambridge, MA, and approved December 26, 2017 (received for review August 10, 2017)

Although the motility of the flagellated bacteria, Escherichia coli, has been widely studied, the effect of viscosity on swimming speed remains controversial. The swimming mode of wild-type E. coli is often idealized as a run-and-tumble sequence in which periods of swimming at a constant speed are randomly interrupted by a sudden change of direction at a very low speed. Using a tracking microscope, we follow cells for extended periods of time in Newtonian liquids of varying viscosity and find that the swimming behavior of a single cell can exhibit a variety of behaviors, including run and tumble and "slow random walk" in which the cells move at a relatively low speed. Although the characteristic swimming speed varies between individuals and in different polymer solutions, we find that the skewness of the speed distribution is solely a function of viscosity and can be used, in concert with the measured average swimming speed, to determine the effective running speed of each cell. We hypothesize that differences in the swimming behavior observed in solutions of different viscosity are due to changes in the flagellar bundling time, which increases as the viscosity rises, due to the lower rotation rate of the flagellar motor. A numerical simulation and the use of resistive force theory provide support for this hypothesis.

bacteria | flagella | bundle | fluid mechanics | motility

The survival of motile bacteria depends in part on the ability to navigate their environment, swimming toward attractants (e.g., food) and away from repellents (e.g., toxins). To move in a low Reynolds number environment and to avoid the time reversibility of Stokesian dynamics (1), flagellated bacteria such as Escherichia coli exhibit a nonreciprocal swimming behavior first described by Berg and Brown (2). The "run-and-tumble" behavior is characterized by extended linear movements ("runs") punctuated by sudden changes in direction ("tumbles"). The tumbling event is initiated by the clockwise (CW) rotation of one or more of the flagellar motors (3, 4) (T_o in Fig. 1A). This precipitates the unraveling of the flagellar bundle which causes the cell to immediately stall and reorient ($T_o \rightarrow T_1$). As the motor returns to counterclockwise (CCW) rotation (T_2), the flagellar bundle reforms ($T_2 \rightarrow T_3$) (4, 5) and the cell accelerates back to its characteristic run speed, U_o . Note that the value of U_o can vary and depends on the cell metabolism; the number, length, and spatial distribution of flagella; and the conditions of the surrounding fluid (presence or absence of nutrients, etc.).

This mode of cell motility has been studied extensively over the past decades (6–14) and while it remains a compelling idealized model for multiflagellated motion, there remain questions. For example, Molaei et al. (15) analyzed thousands of individual cell motion histories and reported that only 70% of the *E. coli* cells exhibited a run-and-tumble style of motion while the rest of the cells moved in a different mode, termed "slow random walk" and characterized by a slower average speed and absent clearly defined tumbling events. More recently, a close examination of cell motility and flagellar motion (16) revealed intermediate states, such as partial unbundling, which also contributed to

a wider variety of swimming modalities than the binary run and

Bacteria live in varied fluid environments that can exhibit viscous and/or viscoelastic properties (18); measurements and calculations of cell motility in these complex fluids have yielded seemingly contradictory results and explanations of swimming behavior (13, 14, 19-26). Even for cells swimming in (assumed to be) Newtonian polymer solutions of varying viscosity, the picture is unclear. One of the earliest experimental studies in polymeric solutions shows that the swimming speed is increased even when the polymer concentration is low (19). The authors explain this phenomenon by appealing to the properties of the loose and quasi-rigid polymer network and its interactions with the nanoscale flagellar propulsors. Magariyama and Kudo (27) proposed a simple model based on resistive force theory (RFT) (1), but modified by the introduction of two apparent viscosities that depend on the length, morphology, and interaction between polymer molecules (27). A further complication arises from the observation that the level of biological activity appears to change with the addition of the thickening polymer (13), probably due to the metabolism of small polymer fragments by the bacteria.

To fully understand the different swimming modes, cells must be observed for relatively long time periods and in different fluid environments. Two methodologies are commonly described. In most studies, cells are tracked under a stationary microscope platform (13, 15) which, although effective and straightforward, permits tracking only for short times as the cells quickly pass through the microscope's field of view and focal plane.

Significance

Changes in the swimming speed and behavior of wild-type *Escherichia coli* in Newtonian fluids of varying viscosity are described. Individual cells exhibit both "run-and-tumble" and "slow random-walk" modes of motility. As the solution viscosity rises, variations in the flagellar bundling time account for changes in the swimming behavior of the cells. A unique contribution is the identification of the skewness of the speed distribution as a key parameter for characterizing different swimming behaviors. The skewness is shown to be solely a function of viscosity and independent of the cell's metabolic activity. Using both numerical simulation and resistive force theory, we compute the flagellar bundling time as a function of viscosity and achieve good agreement with direct observations.

Author contributions: Z.Q., F.Z.T., and K.S.B. designed research; Z.Q. and R.H. performed research; Z.Q. and R.H. analyzed data; and Z.Q., F.Z.T., and K.S.B. wrote the paper.

The authors declare no conflict of interest.

This article is a PNAS Direct Submission.

Published under the PNAS license.

¹To whom correspondence should be addressed. Email: zijie_qu@brown.edu.

This article contains supporting information online at www.pnas.org/lookup/suppl/doi:10. 1073/pnas.1714187115/-/DCSupplemental.

Downloaded from https://www.pnas.org by 206.237.119.212 on August 6, 2025 from IP address 206.237.119.212.

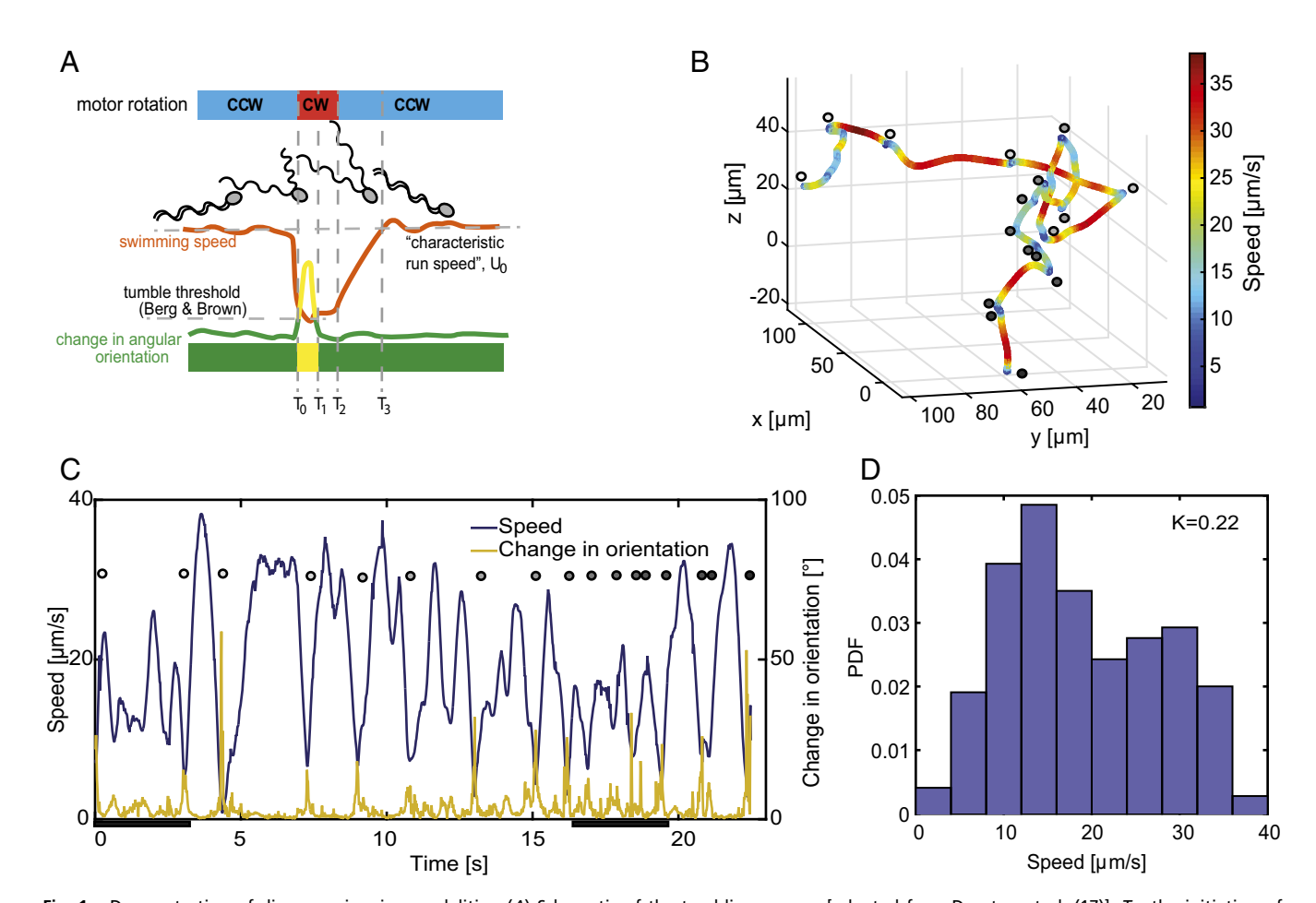


Fig. 1. Demonstration of diverse swimming modalities. (A) Schematic of the tumbling process [adapted from Darnton et al. (17)]. To, the initiation of tumble when motor starts to rotate CW; T_1 , the end of tumble according to the definition given by Berg and Brown (2); T_2 , the motor starts to rotate CCW and the rebundling is initiated; T_3 , the completion of the bundle process when the swimming speed reaches the characteristic run speed U_o . (B) The 3D trajectory of a representative E. coli cell swimming in 1.25% native Ficoll 400 solution (1.17 cP). Color change denotes the speed of the cell. (C) Time history of swimming speed (blue) and change in orientation (yellow). The circles in both B and C denote a tumble event, using the definition of Berg and Brown (2). Circles with the same color refer to the same event. The black bars on the x axis of C identify periods of slow random walk (15). (D) The corresponding probability distribution function of the swimming speed. The two peaks at 12 µm/s and 30 µm/s correspond to the slow random-walk and run motilities.

Alternatively, one can track individual cells in three dimensions by physically moving the objective and the microscope stage in real time (2, 16, 28). Although the tracking microscope is inefficient in terms of the number of observed individuals, the extended tracking time permits detailed observation of similarities and differences in the swimming behavior both for a single cell and between individual cells in an identical genetic population.

În this article, in an attempt to understand the different swimming modalities and the role of viscosity on cell motility, we report on the use of tracking microscopy to measure the detailed behavior of wild-type E. coli swimming in Newtonian fluids of varying viscosity. Solutions of polymers using two molecular weights were prepared, and cell trajectories in both native and dialyzed polymer solutions were recorded.

Results and Discussion

A typical time history of speed and angular change (Fig. 1 B and C) shows good qualitative and quantitative agreement with the classic results of Berg and Brown (2). Using their definition of the run-and-tumble phases (Fig. 1A), we find that the run time and tumbling frequency are not affected by the fluid properties (Table 1). This is in contrast to the recent results of Patteson et al. (14) who observed that both the mean run and tumble times increased with viscosity, suggesting that the frequency with the flagellar motor changes its sense of rotation decreases with viscosity. However, the CW and CCW motor rotation intervals are relatively insensitive to viscosity as long as the motor operates above a low speed nearing stall ($\omega > 50$ Hz) and below the no-load conditions ($\omega < 250$ Hz) (29, 30). While the viscosity of the fluids considered by Patteson et al. (14) was as high as 19 cP—conditions that would put the motor frequency below 50 Hz—the present experiments were conducted in buffer solutions whose viscosity never rose above 5 cP (Table 1). In this regime, the motor rotation speeds are quite moderate and hence the motor reversal rates can be assumed to be independent of viscosity.

The change in fluid viscosity also has no effect on the change in orientation experienced during a tumble (Table 1). Although a more viscous fluid does imply a reduced angular diffusivity (31, 32), the cell reorientation is an active, not passive event, driven by the splayed flagella pointing and rotating in different directions. During the tumble, a rotation of 1 rad is achieved in roughly 0.1 s (Table 1). In contrast, at the lowest viscosity, a 1-rad diffusive rotation $(t \sim \theta^2/2D_r)$ (32) would take approximately 50 times longer. The detailed mechanics of the tumble remain a complex problem, particularly since one or more flagella might even have a different polymorphic shape (curly, semicoiled, normal, etc.), depending on their sense of rotation and the applied torque (17).

Table 1. Run-and-tumble statistics in different polymers at different viscosities

Solution or buffer, %	Viscosity, cP	Run time, s	Tumble time, s	Tumble angle, $^\circ$	Mean tracking time, s	No. of cells
MB 0.00	0.93	0.88 ± 0.06	0.13 ± 0.01	71.72 ± 4.79	14.49 ± 0.48	28
F70						
1.67	1.06	1.00 ± 0.02	0.11 ± 0.01	69.52 ± 4.21	16.63 ± 0.72	27
2.00	1.11	$\textbf{0.85} \pm \textbf{0.02}$	$\textbf{0.13} \pm \textbf{0.01}$	74.01 ± 3.11	14.37 ± 0.89	23
2.22	1.15	$\textbf{0.81} \pm \textbf{0.03}$	$\textbf{0.13} \pm \textbf{0.01}$	75.03 ± 4.26	19.46 ± 1.47	27
3.33	1.24	$\textbf{0.83} \pm \textbf{0.09}$	$\textbf{0.14} \pm \textbf{0.02}$	74.30 ± 2.33	18.41 ± 1.15	28
6.67	1.76	$\textbf{0.81} \pm \textbf{0.03}$	$\textbf{0.15} \pm \textbf{0.01}$	84.60 ± 4.38	18.56 \pm 1.55	25
10.00	2.52	$\textbf{0.92} \pm \textbf{0.04}$	$\textbf{0.14} \pm \textbf{0.01}$	68.84 ± 5.10	15.36 \pm 0.91	27
F70Di						
1.00	1.01	$\textbf{0.96} \pm \textbf{0.04}$	$\textbf{0.11} \pm \textbf{0.02}$	70.37 ± 4.13	17.42 ± 0.91	28
2.50	1.17	$\textbf{0.90} \pm \textbf{0.06}$	$\textbf{0.13} \pm \textbf{0.02}$	67.93 ± 4.46	18.07 ± 0.83	26
3.33	1.24	$\textbf{0.89} \pm \textbf{0.08}$	$\textbf{0.12} \pm \textbf{0.02}$	69.95 ± 5.58	17.87 ± 0.98	23
5.00	1.50	$\textbf{0.97} \pm \textbf{0.06}$	$\textbf{0.12} \pm \textbf{0.02}$	73.54 ± 3.51	17.13 ± 1.22	25
6.67	1.76	$\textbf{0.86} \pm \textbf{0.05}$	0.11 ± 0.01	64.88 ± 4.78	18.41 ± 1.06	23
10.00	2.52	$\textbf{0.93} \pm \textbf{0.10}$	0.11 ± 0.03	69.29 ± 7.62	15.84 \pm 1.11	22
F400						
0.83	1.11	1.00 ± 0.06	0.11 ± 0.01	69.07 ± 2.94	16.38 ± 1.08	28
1.25	1.17	$\textbf{0.99} \pm \textbf{0.11}$	$\textbf{0.13} \pm \textbf{0.02}$	65.42 ± 3.57	16.74 ± 0.82	24
1.67	1.25	$\textbf{0.89} \pm \textbf{0.08}$	$\textbf{0.12} \pm \textbf{0.01}$	68.89 ± 4.32	14.52 ± 0.81	22
2.00	1.32	$\textbf{0.91} \pm \textbf{0.13}$	$\textbf{0.14} \pm \textbf{0.01}$	$\textbf{78.84} \pm \textbf{4.50}$	$\textbf{13.34} \pm \textbf{0.70}$	24
2.22	1.37	$\textbf{0.82} \pm \textbf{0.07}$	$\textbf{0.13} \pm \textbf{0.01}$	74.45 ± 3.32	16.27 ± 0.80	22
3.33	1.61	$\textbf{0.99} \pm \textbf{0.11}$	$\textbf{0.13} \pm \textbf{0.01}$	73.93 ± 6.19	15.12 ± 1.37	21
6.67	2.73	$\textbf{0.89} \pm \textbf{0.05}$	$\textbf{0.14} \pm \textbf{0.02}$	67.86 ± 8.64	14.19 ± 1.07	22
10.00	4.85	$\textbf{0.89} \pm \textbf{0.10}$	$\textbf{0.14} \pm \textbf{0.02}$	73.99 ± 4.19	14.98 ± 1.02	23
F400Di						
0.83	1.11	0.95 ± 0.10	0.11 ± 0.02	60.20 ± 4.38	14.41 ± 0.62	29
1.25	1.17	$\textbf{0.88} \pm \textbf{0.11}$	$\textbf{0.10} \pm \textbf{0.02}$	66.56 ± 7.21	14.06 ± 0.69	23
2.00	1.32	$\textbf{0.80} \pm \textbf{0.11}$	$\textbf{0.11} \pm \textbf{0.02}$	65.14 ± 3.77	14.81 ± 0.66	22
3.33	1.61	$\textbf{0.95} \pm \textbf{0.11}$	$\textbf{0.12} \pm \textbf{0.02}$	69.08 ± 4.56	15.13 ± 0.78	24
6.67	2.73	$\textbf{0.92} \pm \textbf{0.10}$	$\textbf{0.12} \pm \textbf{0.02}$	70.43 ± 3.41	16.53 ± 0.72	25
10.00	4.85	$\textbf{0.90} \pm \textbf{0.06}$	$\textbf{0.13} \pm \textbf{0.02}$	76.04 ± 4.37	16.30 ± 1.27	24

F70 and F400, Ficoll 70 and Ficoll 400 native solutions; F70Di and F400Di, dialyzed solutions; MB, motility buffer. The concentration is wt/vol %.

Speed Distribution and Skewness. A close inspection of the time traces (Fig. 1 B and C) indicates that the run-and-tumble description of motility may be too idealized to represent the observed swimming history; we see that a single cell exhibits both classical run-and-tumble events and periods of extended low-speed swimming or slow random walk (15). This is quantitatively reflected by the probability density function (PDF) of the swimming speed during a single-cell tracking sequence (Fig. 1D) which shows two peaks: one at high speed, which we associate with the observed run behavior, and a second peak at a lower speed, corresponding to the slow random-walk behavior.

From these results, we assert that the slow random-walk mode of motility is not the result of different cells illustrating different swimming modalities. Rather, over an extended period, a single cell can exhibit multiple modes of motility. Indeed, more complex combinations of speed and orientation changes are observed, (e.g., Fig. 1C, $t \approx 0\text{--}4$ s), which might be due to partial unbundling (16).

A valuable means to quantify differences between swimming behaviors is given by the shape of an individual cell's speed (U) distribution during a tracking sequence. In particular, the skewness, $K = \overline{(U-\overline{U})^3/\sigma^3}$, where the overbar denotes the mean

ness, $K = \overline{(U-\overline{U})^3/\sigma^3}$, where the overbar denotes the mean value and σ is the sample standard deviation, is independent of the magnitude of the swimming speed and can illustrates a coexistence between run-and-tumble and slow random-walk behaviors. One can imagine that a swimmer exhibiting a pure run-and-tumble behavior would have a PDF characterized by a sharp peak at the run speed with a broad low-speed tail. Such a speed distribution would have a negative skewness (K < 0). Similarly, a cell that spends more time in a tumbling state, with only short

runs, would have a low mean speed and a positively skewed PDF (K > 0). Extreme swimming behaviors exhibited by mutant strains would also have characteristic speed distributions. For example, a "smooth" swimmer (one that does not tumble) would have a PDF with a peak at a high speed and zero skewness, while a "tumbly" swimmer—a cell that tumbles continuously—would have a speed distribution with a low mean speed and zero skewness.

The independence of the skewness to the magnitude of the average swimming speed is also of great value to the analysis of the data. Even though the average run times and tumble frequencies are relatively constant (Table 1), there is considerable cellto-cell variation in absolute swimming speed (the standard deviation, σ is approximately five times larger than the standard error bars plotted in Fig. 2A), most likely due to natural variations in the cell size, the length and number of flagella, and/or individual variations in metabolic level. In addition, we observe that there is a marked difference between the swimming speeds in dialyzed and native polymer solutions despite the fact that these solutions have the same bulk viscosity. Although the average swimming speed does decrease as viscosity rises, there does not appear to be a uniform behavior. The average swimming speed in native solutions increases initially before decaying, a phenomenon that has been previously observed (19, 27, 33). However, in dialyzed solutions, the average swimming speed decays monotonically as viscosity rises. This discrepancy between average swimming speeds in native and dialyzed media was also observed by Martinez et al. (13) who attributed the difference to the presence of polymer fragments in the native solution that increase the baseline cell metabolic rate and motility.

Downloaded from https://www.pnas.org by 206.237.119.212 on August 6, 2025 from IP address 206.237.119.212.

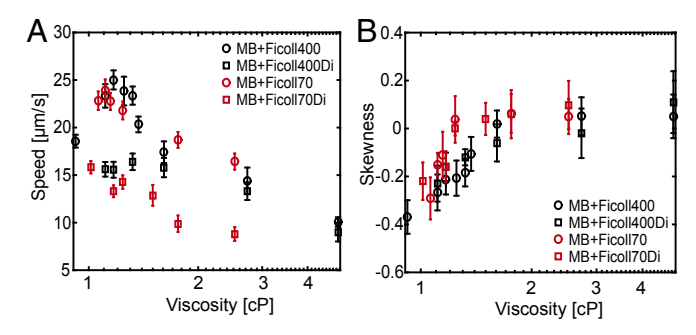


Fig. 2. (A) Average swimming speed as a function of viscosity for Ficoll 400 and Ficoll 70 solutions (native and dialyzed). (B) Skewness of the swimming speed distribution as a function of viscosity. Although the average swimming speed exhibits variations as a function of the viscosity and the specific polymer solution, the skewness of the swimming speed distribution demonstrates a unified behavior, depending only on viscosity. The values in A and B are the mean \pm 1 standard error (σ/\sqrt{N}) . In the calculation of the mean speed and mean skewness, each bacterium is weighted equally. The average swimming speed of each bacterium is a time-averaged speed without trying to distinguish between run and tumble.

Characterizing motility purely by the average swimming speed thus appears to be too blunt a tool; however, looking at the skewness of the speed distributions (Fig. 2B) we see that as the viscosity increases, the skewness changes monotonically, reflecting a shift from a predominantly run-and-tumble style, characterized by a negative skewness, to a predominantly slow random-walk style of swimming, characterized by a skewness close to zero. The same behavior is observed in all four polymer solutions (two different molecular weights, dialyzed and native solutions). This suggests that the shape of the speed distribution is a reliable fingerprint of the cell's swimming behavior, even while the mean value can show variability.

Note that the long-time speed histories of individual cells recorded using the tracking microscope provide the ability to generate these individual cell speed distributions. Population speed distributions, assembled by aggregating measurements from many cells (34, 35) will have a different shape (see SI Text for more details and examples).

The Effects of Viscosity on the Bundling Time. What might be the cause of this change in the swimming speed distribution? Assuming that the geometry of the cell body and flagellar filaments does not depend on the fluid viscosity, the hydrodynamics of the run scale linearly with viscosity (1, 31). Furthermore, the run-and-tumble durations are independent of viscosity (Table 1). However, the time for the flagellar bundle to unravel and reform during the tumble does change with viscosity. Kim et al. (5) showed that the flagellar bundling of elastic helices depends on a nondimensional parameter, $M = \mu \omega L^4 / EI$, where μ is the fluid viscosity, ω is the rotation rate, L the filament length, E the elastic modulus, and I the moment of inertia. M represents the balance between the viscous and elastic stresses in the filament and Kim et al. (5) demonstrated that flagellar bundling occurs after about 15 rotations for values of M greater than about 100. For a fixed torque motor (17, 36), the flagellar rotation rate will decrease as the fluid viscosity increases, indicating that the bundling process, which requires a fixed number of rotations (5), will take longer at higher viscosity. In addition, Turner et al. (4) observed that the swimming speed of the cell remains depressed after tumble due to the rebundling process. Thus, it seems plausible that, as the viscosity rises, the cell spends less time running at full speed and more time at lower speed recovering from tumbles. This hypothesis is consistent with our observation that the speed distribution skewness approaches or passes zero as the viscosity rises (Fig. 2B, SI Text, and Fig. S3). The effect is obscured in the speed vs. viscosity data (Fig. 24) by the confounding factors of individual variations in cell morphology and metabolic activity as well as the effects of polymers on cell activity level.

Numerical Simulations. A numerical simulation confirms the relationship between the bundling time, the scaled average speed, and the skewness of the speed distribution. We model the swimming as a combination of a run at a given "characteristic run speed," U_o (18 µm/s), punctuated by tumbles that occur randomly. The acceleration from the tumble back to U_o is changed by the effect of varying viscosity on the bundling dynamics.

Using this idealized simulation, we generate synthetic speed histories and speed distributions associated with different bundling times (Fig. 3 A and B) that are both qualitatively and quantitatively similar to the experimentally measured distributions (e.g., Fig. 1D). From the simulated speed histories, we plot the distribution skewness against the ratio of the average swimming speed to the characteristic run speed, \overline{U}/U_o , and find that the data exhibit a linear trend: $\overline{U}/U_o = 0.627 - 0.185K$ (Fig. 3C). More importantly, the simulation results allow us to use measurements of the speed distribution skewness, K, and the average swimming speed, \overline{U} , to estimate the characteristic run speed, U_o —a parameter that varies from cell to cell and is difficult to measure directly.

Evaluation of Motor Torque and Bundling Time. With the estimate for U_o , and typical values for the geometry of the cell and flagella (SI Text and Table S1), we use RFT to calculate the motor torque, τ , as well as the cell and flagellar rotation rates, ω_c and ω_f , respectively, (see *SI Text* for details). Although there is scatter in the data, the motor torque (at stall) is estimated to lie between 0.25×10^{-18} Nm and 0.75×10^{-18} Nm (Fig. 4A), which agrees well with the measurement of Darnton et al. (17) who used a similar technique, but is lower than the measurement of Reid et al. (37). It is worthwhile to note that the motor torque in the native polymer solutions is higher than the torque in the dialyzed solutions (Fig. 4A, circles and squares, respectively),

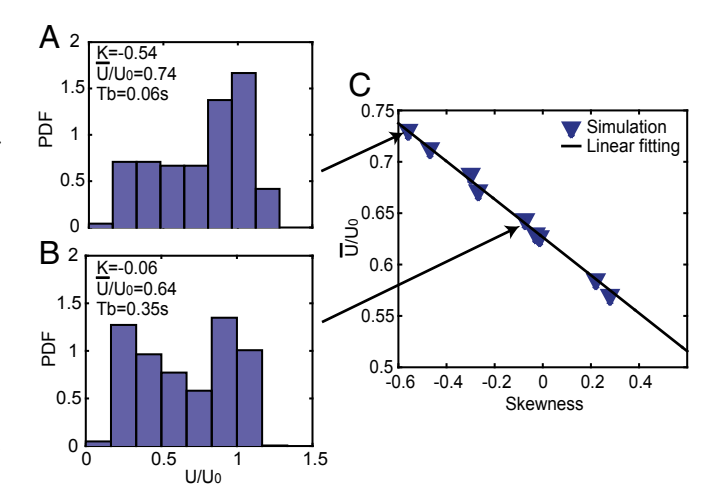


Fig. 3. Idealized numerical simulations of swimming are defined by a characteristic run speed (U_o , held constant at 18 μ m/s), a tumbling frequency (1 Hz), and a bundling time, T_b (varied, to simulate the effects of viscosity on the flagellar bundling process). (A and B) The distribution of swimming speeds for (A) a "pure" run-and-tumble swimmer ($T_b = 0.06$ s, K = -0.54) and (B) a combined swimmer ($T_b = 0.35$ s, K = -0.06) shows the effects of bundling time on the overall distribution. (C) A linear relationship is observed between the skewness of the swimming speed, K, and the ratio of the average speed to characteristic run speed: $\overline{U}/U_0 = -0.185 \times K + 0.627$ (corresponding to 0.06 s $< T_b <$ 0.70 s).

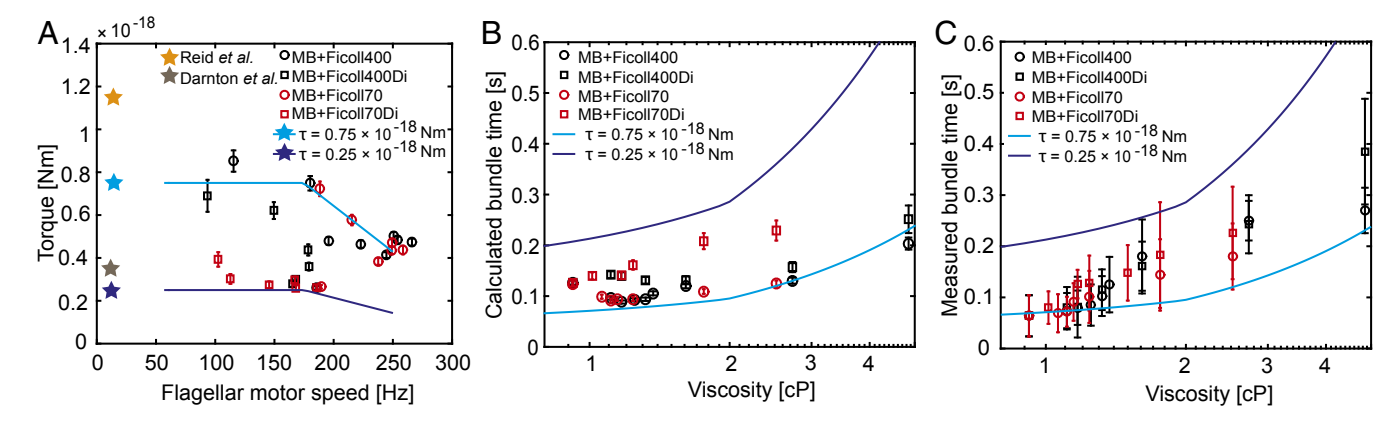


Fig. 4. (A) Flagellar motor torque, calculated using RFT and using the measured characteristic run speed, U_o , and a typical cell geometry (27). The blue solid lines are upper and lower bounds of the torque-speed characteristic, assuming a fixed "knee" speed at 175 Hz (36). Previous motor torque measurement by Reid et al. (37) and Darnton et al. (17) are shown for comparison. (B) Calculated bundling time, T_b , as a function of viscosity. Here the calculations are based on RFT. Flagellar rotation rate ω_f is calculated using the characteristic run speed, U_o , determined from the skewness of the speed distribution from Fig. 3C. T_b is then calculated using ω_f under a fixed number of rotations. (C) Measured bundling time as a function of viscosity. The bundling time is calculated from the swimming histories. In both B and C, the solid lines are calculated from RFT using motor torque characteristics given A.

consistent with the observations both here and by Martinez et al. (13) that the cell activity is generally higher in the native polymer solutions.

Using the motor torque and flagellar rotation rate obtained from RFT, we calculate the bundling time, $T_b = T_3 - T_2$ (Fig. 4B), assuming that 20 rotations are required for complete bundling. The results support the hypothesis that the bundling time is a function of viscosity, rising from ~ 0.1 s in pure motility buffer to about 0.2 s in the most viscous medium.

A second, independent, estimate of the bundling time can be found from the measured speed vs. time history of each cell. To accomplish this, we first use the skewness of the measured speed distribution to determine the characteristic run speed, U_o (Fig. 3C). Using Berg and Brown's definition of a change in angular orientation greater than $35^{\circ}/0.08$ s we identify the start of each tumble (T_o in Fig. 1A) and mark the completion of the rebundling process as the time at which the swimming speed first reaches the characteristic run speed (T_a in Fig. 1A). Since we do not measure T_a , we define the bundling time, T_b as $T_a - T_o - 0.32$, where 0.32 s is used as the duration of the CW rotation, $T_a - T_o$ (Fig. 1A) (3, 4, 17).

The estimate of the flagellar bundling time obtained using this method (Fig. 4C) agrees well with the results obtained using RFT (Fig. 4B), demonstrating that the bundling time increases with viscosity, rising from about 0.08 s to 0.3 s over the fivefold increase in viscosity. The scatter in the data likely results from our inability to accurately estimate the exact duration of the CW rotation, $T_2 - T_o$, and the variability associated with the determination of T_3 .

Summary and Conclusions

We have shown that the motility of a wild-type $E.\ coli$ cell is quite nuanced, exhibiting both run-and-tumble and slow random-walk modes of locomotion. The balance between these natural swimming behaviors can be quantified using both the average speed, \overline{U} , and the skewness of the speed distribution, $K.\ A$ distinct feature of the skewness is that it is independent of differences in the characteristic run speed that arise due to cell-to-cell variations and the uncontrolled presence of biological stimulants in the surrounding medium.

We believe that these results clarify some of the confusion surrounding cell motility in viscous media by demonstrating that the swimming behavior changes as the viscosity rises due to the fact that the flagellar bundling process takes longer at higher

viscosity, slowing the rotation of the flagellar motors. Future experiments, theory, and simulations, including using viscoelastic media (13, 14, 20, 24, 26) and visualizing the flagella (4, 16), will be critical in providing a full understanding of this mechanism.

Materials and Methods

Cell Preparation. The cells used in the experiments were wild-type *E. coli* K12 AW405. A single colony was picked from an agar plate and cultured in 10 mL T-Broth (1 L water, 10 g tryptone, and 5 g NaCl) by rotating at 200 rpm for 16 h at 30 $^{\circ}$ C (Southwest Science, Incu-Shaker Mini). A total of 20 μ L of bacteria suspension was cultured again in 10 mL of T-Broth for 4 h until midexponential growing phase of *E. coli*. The bacterial suspension was washed three times by centrifuging at 2,000 rpm (Eppendorf, MiniSpin Plus) for 8 min and resuspending in fresh motility buffer (1 L water, 11.2 g K2HPO4, 4.8 g KH2PO4, 0.029 g EDTA, 3.9 g NaCl, pH 7–7.5). The final suspension was diluted threefold before conducting experiments.

Polymer Solutions. Ficoll 400 and Ficoll 70 have the same polymer structures, but different molecular weight. The molecular weights of Ficoll 400 and Ficoll 70 are 400,000 and 70,000, respectively. A 10% (wt/vol) stock solution of both Ficoll 400 and Ficoll 70 (Sigma-Aldrich) was prepared by dissolving the polymer in deionized water and rotating overnight at 200 rpm. The polymer solution was dialyzed for 1 wk (Spectra/Por 2 Dialysis Trial Kit; 12–14 kDa molecular-weight cutoff, 23 mm flat-width membrane). The final polymer concentration was calculated by measuring the weight before and after evaporating the solvent for 6 h at 60 °C and placing the solution for 4 h in vacuum until the final weight reaches a constant. The bulk viscosity of the solutions was measured using a rheometer (TA Instruments; AR2000) at different shear rates. Ficoll solution is known to be Newtonian (19) and our measurements confirm that the viscosity is independent of shear rate.

Test Fixture. The cell motion was observed using a test fixture consisting of a "swimming pool" cut from a 2-mm film of polydimethylsiloxane (PDMS) sandwiched by a No. 1 glass slide and a No 1.5 glass cover slide.

Real-Time 3D Digital Tracking Microscopy. A 3D digital tracking microscope was used to observe the swimming behavior of the cells. It allows us to study the motility of individuals for a relatively long period (15 s on average) compared with more common stationary microscope stages. The cells are observed using a Nikon TE200 inverted microscope with a CFI Plan Fluor 20XMI objective and PCO edge 5.5 sCMOS camera. A 2D translational stage (Prior) is used for tracking the cells in the 2D plane parallel to the glass slide. A piezo objective positioner (Physik Instrumente) was used to rapidly control the position of the focal plane in real time so that the cell always remains in the field of view. Images were acquired at 60 fps with a resolution of 640 pixels × 480 pixels. A real-time algorithm, written in C++ and OpenCV,

detects the position (centroid) of a single cell in the image and moves the stage and objective to maintain the cell in focus and within the field of view.

Simulation of Synthetic Swimming Speed Histories. Synthetic swimming speed histories were created using a Matlab code designed to explore the connection between the bundling time and the skewness of the swimming speed distribution. The cell was assumed to swim with a characteristic speed of $U_0 = 18 \mu \text{m/s}$. The duration of each run, in which all flagellar motors are assumed to be rotating in a CCW direction, is sampled from an exponential distribution (3, 16) with an average run time of 0.86 s (2). Following the schematic in Fig. 1A, the tumble is modeled as a rapid deceleration in speed, from U_o to a tumble speed of $U_t = 5 \mu \text{m/s}$ in 0.1 s. The cell remains at U_t for the duration of the tumble, $T_t = T_1 - T_0$, sampled from an exponential distribution with a mean time of 0.14 s. The rebundling process,

- 1. Purcell EM (1977) Life at low Reynolds number. Am J Phys 45:3-11.
- 2. Berg HC, Brown DA (1972) Chemotaxis in Escherichia coli analysed by threedimensional tracking. Nature 239:500-504.
- Berg HC (2008) E. coli in Motion (Springer, New York).
- Turner L, Ryu WS, Berg HC (2000) Real-time imaging of fluorescent flagellar filaments. J Bacteriol 182:2793-2801.
- Kim M, Bird JC, Van Parys AJ, Breuer KS, Powers TR (2003) A macroscopic scale model of bacterial flagellar bundling. Proc Natl Acad Sci USA 100:15481–15485.
- 6. Lighthill J (1976) Flagellar hydrodynamics. SIAM Rev 18:161-230.
- Hotani H (1982) Micro-video study of moving bacterial flagellar filaments: III. Cyclic transformation induced by mechanical force. J Mol Biol 156:791–806.
- Berg HC, Turner L (1993) Torque generated by the flagellar motor of Escherichia coli. Biophys J 65:2201-2216.
- Berg HC, Turner L (1995) Cells of Escherichia coli swim either end forward. Proc Natl Acad Sci USA 92:477-479.
- 10. Fraser GM, Hughes C (1999) Swarming motility. Curr Opin Microbiol 2:630-635.
- 11. Powers TR (2002) Role of body rotation in bacterial flagellar bundling. Phys Rev E
- 12. Dalton T, et al. (2011) An in vivo polymicrobial biofilm wound infection model to study interspecies interactions. PLoS One 6:e27317.
- Martinez VA, et al. (2014) Flagellated bacterial motility in polymer solutions. Proc Natl Acad Sci USA 111:17771-17776.
- Patteson A, Gopinath A, Goulian M, Arratia P (2015) Running and tumbling with E.
- coli in polymeric solutions. Sci Rep 5:15761. Molaei M, Barry M, Stocker R, Sheng J (2014) Failed escape: Solid surfaces prevent tumbling of Escherichia coli. Phys Rev Lett 113:068103.
- 16. Turner L, Ping L, Neubauer M, Berg HC (2016) Visualizing flagella while tracking bacteria. Biophys J 111:630-639.
- 17. Darnton NC, Turner L, Rojevsky S, Berg HC (2007) On torque and tumbling in swimming Escherichia coli. J Bacteriol 189:1756-1764.
- 18. Kimsey RB, Spielman A (1990) Motility of Lyme disease spirochetes in fluids as viscous as the extracellular matrix. J Infect Dis 162:1205-1208.
- 19. Berg HC, Turner L (1979) Movement of microorganisms in viscous environments. Nature 278:349-351.

 $T_{bsim} = T_3 - T_1 = T_b + 0.32 - T_t$, is modeled as a linear recovery in speed after tumble where 0.32 s is the duration of CW rotation (3, 4, 17). Simulations were performed with T_b ranging from 0.06 s to 0.70 s, mimicking the change in the viscosity. Characteristic run-and-tumble speeds are held constant throughout the simulation since the statistics remain unchanged with linearly changed U_0 and U_t as a result of change in viscosity. The run-tumble cycle is repeated to generate a time series lasting 2.000 s. Finally, Gaussian white noise is added (1 dBW) to the entire series, representing measurement uncertainty and diffusivity.

ACKNOWLEDGMENTS. We are grateful to Coli Genetic Stock Center (Yale University) for strains and advice. We thank Anubhav Tripathi for the help in measuring the sample viscosity and Liza Gibbs for assistance with culturing E. coli. This work was supported by the National Science Foundation (Chemical, Bioengineering, Environmental, and Transport Systems no. 1336638).

- 20. Lauga E (2007) Propulsion in a viscoelastic fluid. Phys Fluids 19:083104.
- 21. Fu HC, Powers TR, Wolgemuth CW (2007) Theory of swimming filaments in viscoelastic media. Phys Rev Lett 99:258101.
- 22. Leshansky A (2009) Enhanced low-Reynolds-number propulsion in heterogeneous viscous environments. Phys Rev E 80:051911.
- 23. Liu B, Powers TR, Breuer KS (2011) Force-free swimming of a model helical flagellum in viscoelastic fluids. Proc Natl Acad Sci USA 108:19516-19520.
- 24. Spagnolie SE, Liu B, Powers TR (2013) Locomotion of helical bodies in viscoelastic fluids: Enhanced swimming at large helical amplitudes. Phys Rev Lett 111:068101.
- 25. Dasgupta M, et al. (2013) Speed of a swimming sheet in Newtonian and viscoelastic fluids. Phys Rev E 87:013015.
- Balin AK, Zöttl A, Yeomans JM, Shendruk TN (2017) Biopolymer dynamics driven by helical flagella. Phys Rev Fluids 2:113102.
- 27. Magariyama Y, Kudo S (2002) A mathematical explanation of an increase in bacterial swimming speed with viscosity in linear-polymer solutions. Biophys J 83:733-739.
- 28. Liu B, et al. (2014) Helical motion of the cell body enhances Caulobacter crescentus motility. Proc Natl Acad Sci USA 111:11252-11256.
- Fahrner KA, Ryu WS, Berg HC (2003) Biomechanics: Bacterial flagellar switching under load. Nature 423:938.
- Yuan J, Fahrner KA, Berg HC (2009) Switching of the bacterial flagellar motor near zero load. J Mol Biol 390:394-400.
- 31. Lauga E, Powers TR (2009) The hydrodynamics of swimming microorganisms. Rep Prog Phys 72:096601.
- 32. Berg HC (1993) Random Walks in Biology (Princeton Univ Press, Princeton).
- Schneider WR, Doetsch R (1974) Effect of viscosity on bacterial motility. J Bacteriol 117:696-701.
- 34. Schwarz-Linek J, et al. (2012) Phase separation and rotor self-assembly in active particle suspensions. Proc Natl Acad Sci USA 109:4052-4057.
- 35. Nossal R, Chen SH, Lai CC (1971) Use of laser scattering for quantitative determinations of bacterial motility. Opt Commun 4:35-39.
- 36. Chen X, Berg HC (2000) Torque-speed relationship of the flagellar rotary motor of Escherichia coli. Biophys J 78:1036-1041.
- Reid SW, et al. (2006) The maximum number of torque-generating units in the flagellar motor of Escherichia coli is at least 11. Proc Natl Acad Sci USA 103:8066-8071.